haematologica
Journal of the Ferrata Storti Foundation

Differences in venous clot structures between hemophilic mice treated with emicizumab *versus* factor VIII or factor VIIIFc

by Thibaud Sefiane, Hortense Maynadié, Carmen Escurola Ettingshausen, Vincent Muczynski, Xavier Heiligenstein, Julien Dumont, Olivier D. Christophe, Cécile V. Denis, Caterina Casari, and Peter J. Lenting

Received: August 23, 2023.
Accepted: November 29, 2023.

Citation: Thibaud Sefiane, Hortense Maynadié, Carmen Escurola Ettingshausen, Vincent Muczynski, Xavier Heiligenstein, Julien Dumont, Olivier D. Christophe, Cécile V. Denis, Caterina Casari, and Peter J. Lenting. Differences in venous clot structures between hemophilic mice treated with emicizumab versus factor VIII or factor VIIIFc.
Haematologica. 2023 Dec 7. doi: 10.3324/haematol.2023.284142 [Epub ahead of print]

Differences in venous clot structures between hemophilic mice treated with emicizumab versus factor VIII or factor VIIIFc

Thibaud Sefiane[1], Hortense Maynadié[1,2], Carmen Escurola Ettingshausen[3], Vincent Muczynski[1], Xavier Heiligenstein[4], Julien Dumont[5], Olivier D. Christophe[1], Cécile V. Denis[1], Caterina Casari[1,6], Peter J. Lenting[1,6]

[1]Laboratory for Hemostasis, Inflammation & Thrombosis, Unité Mixed de Recherche 1176, Institut National de la Santé et de la Recherche Médicale, Université Paris-Saclay, 94276 Le Kremlin-Bicêtre, France

[2]Centre de Référence de l'Hémophilie et des Maladies Hémorragiques Constitutionnelles rares, Hôpital Bicêtre AP-HP, Université Paris-Saclay, Le Kremlin-Bicêtre, France

[3]HZRM Hemophilia Center Rhine-Main, Frankfurt-Mörfelden, Mörfelden-Walldorf, D-64546 Germany

[4]CryoCapCell, 94276 Le Kremlin-Bicetre, France

[5]Collège de France, Centre interdisciplinaire de recherche en biologie (CIRB), Unité Mixed de Recherche 1050, Paris, France

[6]CC & PJL contributed equally to this study

Authorship contributions:

TS, HM, VM, XH, JD and PJL performed experiments and analyzed data; CEE provided patient data; ODC, CVD, CC and PJL designed and supervised the study. All authors contributed to the interpretation of the data. PJL wrote the first draft of the manuscript, and all authors contributed to the editing of the final manuscript.

Running head: Treatment-dependent venous clot structures

Data sharing statement: Data are available upon reasonable request to the corresponding author

Correspondence:

Cécile V. Denis, Inserm U1176, 80 rue du Général Leclerc, 94270 Le Kremlin-Bicetre, France

Tel: +331-49595600; Fax: +33146719472; Email: cecile.denis@inserm.fr

Word count: 3987; **Abstract:** 249; **References:** 35; **Figures:** 7

Funding: This study was supported by a research grant to the institute from Sobi.

Conflict of interest: PJL receives research support (paid to the institute) from Sobi, Roche, Pfizer and Sanofi. XH is co-owner of CryoCapCell.

Abstract

Recombinant factor VIII (rFVIII), rFVIIIFc and emicizumab are established treatment options in the management of hemophilia A. Each has its unique mode of action, which can influence thrombin generation kinetics and therefore also the kinetics of thrombin substrates. Such differences may potentially result in clots with different structural and physical properties.

A starting observation of incomplete wound closure in a patient on emicizumab-prophylaxis led us employ a relevant mouse model in which we noticed that emicizumab-induced clots appeared less stable compared to FVIII-induced clots. We thus analyzed fibrin formation *in vitro* and *in vivo*. *In vitro* fibrin formation was faster and more abundant in the presence of emicizumab compared to rFVIII/rFVIIIFc. Furthermore, the time-interval between the initiation of fibrin formation and factor XIII activation was twice as long for emicizumab compared to rFVIII/rFVIIIFc. Scanning-electron microscopy and immunofluorescent spinning-disk confocal-microscopy of *in vivo* generated clots confirmed increased fibrin formation in the presence of emicizumab. Unexpectedly, we also detected a different morphology between rFVIII/rFVIIIFc- and emicizumab-induced clots. Contrary to the regular fibrin-mesh obtained with rFVIII/rFVIIIFc, fibrin-fibers appeared to be fused into large patches upon emicizumab-treatment. Moreover, fewer red blood cells were detected in regions where these fibrin patches were present. The presence of highly-dense fibrin-structures associated with a diffuse fiber-structure in emicizumab-induced clots was also observed when using super-resolution imaging.

We hypothesize that the modified kinetics of thrombin, fibrin and factor XIIIa generation contribute to differences in structural and physical properties between clots formed in the presence of FVIII or emicizumab.

Introduction

The blood coagulation cascade is a series of highly regulated enzymatic reactions designed to generate thrombin, which is needed to produce fibrin in a timely and spatially correct manner.[1] To achieve this goal, the coagulation cascade consists (amongst others) of thrombin-dependent feedback loops that allow for the amplification of thrombin formation. In addition, thrombin is needed to generate activated factor XIII (FXIIIa), which converts the freshly produced fibrin protofibrils into a covalently-linked network, and activated thrombin-activatable fibrinolysis inhibitor (TAFIa), which delays fibrinolytic degradation of the fibrin network.[2,3] Any disturbance of this complex process may potentially lead to an improperly formed fibrin network. Indeed, thrombin concentration has been shown to be a critical determinant of the fibrin-network structure and its physical properties.[4]

One of the key cofactor proteins in the coagulation cascade is factor VIII (FVIII), the functional absence of which is associated with markedly reduced thrombin formation.[5] The thrombin-activated derivative of FVIII, FVIIIa, functions as a cofactor in the tenase-complex, which participates in the amplifying portion of the coagulation cascade. Within the tenase complex, FVIIIa stimulates the generation of activated factor X (FXa) by the enzyme activated factor IX (FIXa). Its physiological relevance is illustrated by the severe bleeding complications associated with FVIII deficiency, a disorder known as hemophilia A.

To compensate for the deficiency of FVIII in hemophilia A patients, replacement therapy using FVIII concentrates has been the treatment of choice over the last four decades.[6] Prophylactic treatment proved efficient in reducing spontaneous bleedings and subsequent joint damage. Despite its effectiveness, replacement therapy faced a number of disadvantages, including the need for frequent intravenous infusions and an immunologic response leading to the presence of neutralizing allo-antibodies against FVIII. These complications have led to the development of alternative treatment options, such as activated factor VII, extended half-life FVIII variants, gene therapy, and so-called non-factor therapies.[7,8] One non-factor approach that has been approved for clinical use is emicizumab, a bispecific antibody that binds both the enzyme FIXa and its substrate FX, thereby mimicking part of the FVIIIa function.[9,10] Emicizumab allows therefore the generation of a certain amount of thrombin without completely correcting coagulation. Clinical studies have shown marked therapeutic benefit of emicizumab, with average annual bleeding rates being below 2 among patients treated with emicizumab prophylactically.[11] Because of its efficacy and its subcutaneous mode of application, increasing numbers of hemophilia A patients are using emicizumab as prophylactic therapy.[12] Despite this success, it has been reported that about 5% of the patients receiving emicizumab may develop spontaneous or trauma-induced muscle bleeds, which sometimes are difficult to stop and require intensive factor replacement therapy.[13]

It is important therefore to better understand the molecular basis by which emicizumab contributes to coagulation in comparison to FVIII. Indeed, their mode of action is quite different.[14] Both components may differ in the timing by which they start acting and when their activity stops, as well as by the location where they may be acting. A similar point can also be made for extended half-life variants, such as recombinant FVIIIFc (rFVIIIFc), where the presence of the Fc portion may affect FVIII distribution and activation during coagulation. Knowing that thrombin formation requires a time- and spatial-dependent regulation, it is thus of relevance to investigate if and how emicizumab and rFVIIIFc may eventually differ from "classic" FVIII regarding the formation of a fibrin network.

It should be noted, that so far studies on fibrin formation using emicizumab have been restricted to *in vitro* settings.[15-17] Moreover, activity of emicizumab is often examined in global assays, such as thrombin generation assays.[18-22] Although this may provide insight into the potential of emicizumab to stimulate thrombin generation relative to FVIII, it provides little insight into the upstream processes that are required to generate a stable clot.

We have therefore explored *in vivo* clot formation by recombinant FVIII (rFVIII), rFVIIIFc and emicizumab using specific bleeding models and microscopic analysis, with focus on the structure of the fibrin network. We found differences in structural morphology between FVIII- and emicizumab-induced clots. Furthermore, kinetics of fibrin and FXIIIa generation are modified when using emicizumab, which could explain in part the differences in clot structure.

Methods

A description of the experimental procedures can be found in the Supplementary materials.

Ethics statement

Photos from patients' wound were taken during consult, and informed consent was given by the parents for their anonymous use in this study. Animal housing and experiments were performed in accordance with French regulations and the experimental guidelines of the European Community. This project was approved by the local ethical committee of Université Paris-Saclay (Comité d'Ethique en Experimentation Animale n°26, protocol APAFIS#26510-202007061525281 v2).

Patient:

A 2-year-old boy with severe hemophilia A (FVIII <1%) on regular prophylaxis with emicizumab (6 mg/kg every 4 weeks, subcutaneously) experienced a deep laceration at his left foot and a consecutive insufficient wound healing. A more extensive description of the patient is available in the Supplementary materials.

In vitro assays

A description of fibrin formation and FXIIIa generation is available in the Supplementary materials.

In vivo models

A tail vein-transection model has been used in this study, which is described in the Supplementary materials.

Microscopy

The application of spinning disk confocal microscopy, scanning electron microscopy and Stimulated Emission Depletion (STED)-microscopy is described in the Supplementary materials.

Results

Patient

A 2-year-old patient with severe hemophilia A under regular emicizumab prophylaxis for 2 years (6 mg/kg every 4 weeks), experienced a deep laceration at his left foot (Figure 1). The wound was treated with local tranexamic acid application and covered with Steri-strips. Emicizumab prophylaxis continued, and bleeding stopped. However, when Steri-strips were removed after ten days, no wound closure or wound healing had occurred, and the covering clot appeared loose and fragile. Patient then received three consecutive FVIII administrations (66 IU/kg intravenously, followed by 33 IU/kg intravenously at 12-hourly intervals) at day 10 and 11 after injury. Complete wound closure was observed at day 11, and wound healing progressed naturally in the following days.

In vivo clot formation

To further explore clot formation *in vivo*, we compared mice receiving emicizumab, rFVIII or rFVIIIFc using a previously validated mouse model. In this model, mice receive emicizumab in combination with human factors IX and X (100 IU/kg), or a single dose of rFVIII or rFVIIIFc.[23] Subsequently, bleeding is assessed in the tail vein-transection (TVT)-model.[24] At the time of injury, plasma concentrations were 10 IU/dl for rFVIII and rFVIIIFc, *versus* 55 μg/ml for emicizumab. These FVIII concentrations were chosen based on the apparent FVIII-equivalence for emicizumab that we observed in our previous *in vivo* studies.[23] Whereas in vehicle-treated mice, all mice started to rebleed after the initial primary stop, treatment with rFVIII, rFVIIIFc or emicizumab resulted in a permanent arrest of bleeding when the wound remained unchallenged (Figure 2A). Efficient bleeding arrest was accompanied by limited blood loss (Supplementary figure S1). In contrast, when the clot covering the injury was removed at 15 and 30 min after injury, differences in response between FVIII- and emicizumab-treated mice were observed. Mice receiving rFVIII or rFVIIIFc readily stopped bleeding again, whereas emicizumab-treated mice displayed a pattern of frequent spontaneous re-bleeding (Figure 2B). Spontaneous re-bleeds were associated with increased blood loss (Supplementary figure S1). We considered the possibility that levels of factors IX and X had diminished below the necessary threshold to support emicizumab, since their respective half-lives are relatively short in mice (3-5 h) compared to human (>20h).[23] However, re-injection of FIX and FX (100 IU/kg) 5 min before clot removal did not affect bleeding profile or blood loss (Figure 2B, Supplementary figure S1). We also examined if the use of tranexamic acid (10 mg/kg) could improve the phenotype of emicizumab-treated mice. Interestingly, tranexamic acid did not prevent spontaneous re-bleeds after clot removal (Figure 2B, Supplementary figure S1), suggesting that the clot instability is unrelated to

increased fibrinolysis of the fibrin network. In conclusion, these *in viv*o data point to potential differences in clot construction between FVIII- and emicizumab-treated mice.

In vitro fibrin formation

Given that a stable fibrin-network is key to the formation of a stable thrombus, we evaluated if differences in the mode of action between rFVIII and emicizumab could affect upstream fibrin formation. Therefore, *in vitro* experiments using human plasma were performed, in which rFVIII (both 10 IU/dl and 100 IU/dl) or emicizumab (55 μg/ml) were added to fibrinogen-enriched FVIII-deficient plasma (Figure 3A). Fibrin formation was monitored by measuring OD-values at 405nm. In the absence of rFVIII or emicizumab, the lag-time was 32 min, and half-maximal fibrin formation was reached at 42 min (Figure 3B). The addition of rFVIII (10 and 100 IU/dl) dose-dependently shortened the lag-time to 24 and 18 min, with half-maximal fibrin formation being at 33 and 26 min, respectively (Figure 3C-D). Similar data were obtained using rFVIIIFc, indicating that coagulation proceeds similarly for both FVIII variants (Supplementary figure S2). Interestingly, lag-time and time to half-maximal fibrin formation were strongly shortened in the presence of emicizumab, to 6 and 14 min, respectively (Figure 3E). In addition, the maximum OD reached with emicizumab (OD=1.17±0.03; n=6) was higher compared to both rFVIII and rFVIIIFc (OD=0.95±0.06 (n=6) and 0.97±0.08 (n=10), respectively; $p<0.0001$), pointing to rapid and increased fibrin formation. Together, these data suggest that modifying the kinetics of FXa generation affects upstream fibrin formation.

In vitro FXIIIa generation

Since fibrin formation involves two distinct steps following the conversion of fibrinogen into fibrin monomers (non-covalent polymerization of fibrin monomers into protofibrils, and subsequent covalent crosslinking via FXIIIa), we decided to monitor FXIII activation in parallel experiments. FXIIIa activity was detected in all conditions (Figure 3B-E). However, the synchronization between the initiation of fibrin formation and FXIIIa generation varied between the different conditions. In particular, a longer interval was observed between the initiation of fibrin and FXIIIa formation for emicizumab (12±2 min) compared to rFVIII at 100 IU/dl (7±1 min) or 10 IU/dl (4±1 min). Furthermore, more FXIIIa was generated in the presence of emicizumab compared to the presence of rFVIII at 100 IU/dl (0.14 OD/min, 95%CI: 0.13-0.15 OD/min versus 0.12 OD/min, 95%-CI: 0.11-0.13; $p=0.026$), rFVIII at 10 IU/dl (0.10 OD/min; $p<0.0001$) or FVIII-deficient plasma (0.11 OD/min; $p<0.0001$). Thus, relative to fibrin generation, activation of FXIII starts later in the presence of emicizumab compared to rFVIII, while once started, more FXIIIa is formed.

In vivo generation of fibrin: scanning-EM analysis

We next studied whether the *in vitro* differences in the kinetics of fibrin formation were also observed *in vivo* by applying the same TVT-model as described for Figure 2. Tails were collected 10 min after injury (in which bleeding had arrested for all treated mice; Figure 2), and tissue sections were prepared for whole-mount scanning-EM, which permits visualizing the outer portion of the clot (Figure 4A). rFVIII-derived clots contained a fibrin-network in which thin, tubular-shaped fibers with homogenous thickness were in a regular mesh over the clot, and cellular components were evenly distributed (Figure 4B). Similar structures were also observed in tail fragments obtained from wild-type mice, whereas FVIII-deficient mice displayed a disturbed network with less fibrin and fiber that had a 1.4-fold increased diameter size ($p=0.032$; Supplementary figure S3). The emicizumab-derived clots were characterized by a completely different fibrin morphology. They consisted of thick and uneven fiber structures that seemed to fuse together, thereby forming large layered structures. Strikingly, these patch-like structures were almost devoid of cellular components, and included small and large circular-shaped holes (Figure 4C). We analyzed these images using ImageJ-software for four different parameters: fibrin coverage, fiber diameter, number of pores and number of intersections (Figure 4D-G). In line with the *in vitro* fibrin generation experiments, more fibrin was detected in emicizumab-treated compared to rFVIII-treated mice (42±8% vs 24±8% *per* field; $p<0.0001$; Figure 4D). The average diameter of the fibrin fibers was also significantly increased 1.8-fold in emicizumab-treated mice (average of 534±90 nm versus 292±101 nm; $p<0.0001$; Figure 4E). Furthermore, there were 2-fold less pores in emicizumab-derived clots compared to rFVIII-derived clots (119±45 versus 248±58 *per* field; $p<0.0001$; Figure 4F). Finally, 1.7-fold more intersections per field of view were detected in rFVIII-induced clots compared to emicizumab-induced clots (11078±2935 versus 6510±1157 *per* field; $p<0.0001$; Figure 4G). These data indicate that clots derived from mice receiving emicizumab are having a different structure from clots generated in mice receiving rFVIII.

In vivo generation of fibrin: spinning-disk confocal immunofluorescence-analysis

To investigate whether differences in fibrin formation were also occurring within the interior of the injury, we first performed spinning-disk confocal imaging using anti-fibrin antibodies (Figure 5A). Five mice were analyzed for each group, with two tissue sections/mouse, and representative images are provided for each condition (wild-type mice, FVIII-deficient mice, and FVIII-deficient mice treated with rFVIII, rFVIIIFc or emicizumab; Figure 5B-F). Similar amounts of fibrin (in terms of mean fluorescence intensity) were found in clots from rFVIII- and rFVIIIFc-treated mice compared to wild-type mice (Figure 5G). This parameter did not further increase with higher doses of rFVIII or rFVIIIFc (500 IU/dl; Supplementary figure S4). Unexpectedly, the mean fluorescence intensity was significantly increased in clots from

emicizumab-treated mice (0.66±0.30 *versus* 0.14±0.05, 0.17±0.10 & 0.26±0.09 for emicizumab, rFVIII, rFVIIIFc & wild-type mice, respectively; p<0.0001; Figure 5B-F). These data are in line with our *in vitro* data, which showed that fibrin formation is more abundant in the presence of emicizumab compared to FVIII.

In vivo generation of fibrin: Stimulated emission depletion (STED)-Microscopy

Although spinning-disk confocal imaging allowed for the quantitative analysis of fibrin formation within the interior clot area, its resolution is insufficient to detect potential differences in structure. We therefore proceeded to perform STED-microscopy, a form of super-resolution microscopy, which is less suited for quantitative analysis of large regions, but enables imaging with sub-diffraction resolution of ≤50 nm. Detailed images of fibrin structures at the interior of the clot were obtained for wild-type, FVIII-deficient and rFVIIIFc- and emicizumab-treated mice (Figure 6A). As expected, typical fiber-like structures similar to those observed using scanning-EM, were readily distinguished in the clots of wild-type, FVIII-deficient and rFVIIIFc-treated mice. The fibrin-mesh was characterized by a homogeneous thickness of the fibers (Figure 6B-D). Interestingly, in each of the images (obtained from three different mice), intense-stained dot-like structures were observed, which for convenience we like to refer to as focal points. With regard to the structures observed in emicizumab-treated mice, fiber-like structures were also present, (Figure 6E). However, these appeared more diffuse and less homogenous in thickness. In addition, the number of focal points was considerably increased in these clots. When calculating the number of focal points using specific ImageJ-software, it was found that on average twice as many focal points were observed in emicizumab-derived clots compared to those under other conditions (0.36±0.12 for emicizumab *versus* 0.18±0.07, 0.21±0.08 & 0.18±0.08 for wild-type, FVIII-deficient and rFVIIIFc-treated mice, respectively (p<0.0001; Figure 6F). Together, these data are in support of the different fibrin structures that are being generated when using emicizumab in comparison to FVIII.

Discussion

There have been anecdotal communications on unusual bleeding episodes in patients using emicizumab. Here, we provide one example in which a laceration in the foot of a 2-year-old severe hemophilia A patient on emicizumab-prophylaxis was characterized by compromised wound closure and healing. This complication was readily corrected upon treatment with FVIII. Although this single example surely is not representative for the majority of hemophilia patients, it is noteworthy that Batsuli *et al.* reported that about 5% of patients on emicizumab prophylaxis develop spontaneous or trauma-induced muscle bleeds requiring intensive factor replacement-therapy.[13] These observations may originate from emicizumab being a less efficient cofactor than FVIIIa for FIXa. Also, they may point to fundamental differences in how clots are generated in the presence of FVIII or emicizumab.

Based on the differences in functionality between FVIII and emicizumab, we have now explored fibrin formation and structure in the presence of rFVIII or rFVIIIFc *versus* emicizumab. Our data demonstrate that there is a difference not only in the amount of fibrin that is generated, but also in the structure of the fibrin-network that is formed.

To consistently asses clot structures *in vivo*, a bleeding model was used that involves the guided transection of the caudal vein, *ie.* the tail vein-transection model (TVT). The advantage of this model lies in the reproducibility by which the injury is made using a specific template.[24] FVIII-deficient mice are an established model to assess the hemostatic efficiency of FVIII and variants thereof.[25,26] In contrast, less information exists with regard to the use of emicizumab in FVIII-deficient mice, because emicizumab is unable to bind to murine factors IXa and X. To overcome this limitation, we previously developed a protocol involving the co-infusion of human factors IX and X, allowing to test the functionality of emicizumab in FVIII-deficient mice.[23] Importantly, we showed that addition of human FIX and FX did not alter hemostasis in FVIII-treated mice, and that human FIX was as functional as murine FIX in *in vitro* clotting assays using murine plasma. In the tail clip-model, emicizumab (55 μg/ml) significantly reduced blood loss, with an efficacy that was similar to FVIII plasma concentrations of about 10 IU/dl. These concentrations were therefore used in the present study.

rFVIII, rFVIIIFc and emicizumab were similar in that they all corrected bleeding in FVIII-deficient mice in the TVT-model (Figure 2). Bleeding stopped shortly after injury, and no spontaneous rebleeding was observed. In contrast, when clots were removed, emicizumab-treated mice displayed a pattern of frequent re-bleeds that was absent in rFVIII- or rFVIIIFc-treated mice. Control experiments verified that the re-bleeds were not due to an absence of human FIX or FX at the time of clot removal. Also increased fibrinolysis was excluded, since the use of tranexamic acid was unable to prevent these re-bleeds. Moreover, preliminary data presented by Locke *et al.*, suggest that clot-lysis time of emicizumab-induced clots is

prolonged 1.6-fold when comparing FVIII-induced clots.[27] Our *in vivo* data suggest the formation of instable clots when using emicizumab.

With fibrin being key in stabilizing wound-covering clots, we focused the rest of this study on fibrin network formation. We realize that other factors, in particular platelet activation and aggregation, are also of relevance to maintain clot stability. We are currently investigating this specific aspect as part of a separate study. When examining unbiased fibrin formation using human FVIII-deficient plasma spiked with rFVIII or emicizumab, it was clear that fibrin generation was quickest in the presence of emicizumab, and also more fibrin was generated (Figure 3). Increased and more rapid fibrin formation is also compatible with the hyper-reactivity of emicizumab in standard aPTT-assays, which rely on fibrin clot formation.[28] One possible explanation for increased and accelerated fibrin formation is related to the different kinetics by which FVIII and emicizumab stimulate coagulation. Emicizumab will promote FXa generation as soon as FIXa becomes available. In contrast, rFVIII (or rFVIIIFc) requires feedback activation by thrombin before it will exert its cofactor function. The modified kinetics in turn alter the kinetics by which thrombin is able to activate its various substrates, including fibrinogen and FXIII.[29,30] The observation that emicizumab accelerates fibrin formation is not limited to the *in vitro* experiments, but is also detected *in vivo*. Two independent microscopic approaches (scanning-EM and immunofluorescent spinning-disk confocal imaging) revealed an excess of fibrin in emicizumab-treated mice compared to FVIII-treated mice (Figures 4 & 5). Moreover, a significant correlation between *in vitro* and *in vivo* fibrin formation was observed, irrespective whether scanning-EM or immunofluorescent spinning-disk confocal imaging was used (Figure 7).

To get insight in the structure of the *in vivo* generated fibrin network, we used two different microscopic techniques. By using scanning-EM, we were able to visualize the outer region of the clot, *ie* the portion that covers the injury. Unexpectedly, we observed quite an unusual fibrin-network in the clots of emicizumab-treated mice. In contrast to individual intertwined fibers that are present in the structures of clots from wild-type mice and FVIII-treated mice, fibrin-fibers appeared to be fused into large patches, with few individual fibers present. Consequently, average diameters were found to be excessively large (>500 nm; Figure 4). In addition, the presence of those patches seems to prevent the inclusion of red blood cells in these areas, resulting in a less dense clot structure.

Also, when using super-resolution (STED)-microscopy to study the interior of the clot, obvious differences were present between FVIII- and emicizumab-dependent clots (Figure 6). A normal fibrin mesh was found in the clots of FVIII-treated mice, whereas a less recognizable fibrin-staining was detected in the clots of emicizumab-treated mice. For the latter, very large, diffusely-stained patterns were observed, characterized by a large number of intense spots, which we referred to as focal points. As for now, we have no information

what these focal points represent in terms of fibrin structure, but they could correspond to the patches we have seen in the scanning-EM images. Another possibility is that these spots represent fibrin that is accumulated at the surface of platelets that are captured in the fibrin network. Additional studies will be performed to get more insight into this aspect.

An intriguing question is what causes the formation of such unusual fibrin-networks under the influence of emicizumab? We observed that the synchronization between fibrin formation and FXIII activation was different between emicizumab and FVIII. The interval between the initiation of fibrin and FXIIIa formation was longer when using emicizumab compared to FVIII (Figure 3). This suggests that the non-covalent polymerization of fibrin profibrils continues over a longer period before FXIIIa starts making the covalent connections. Furthermore, FXIIIa generation was more efficient in the presence of emicizumab, indicating that larger amounts of FXIIIa are available and more covalent connections can be made. These changes in kinetics could potentially contribute to the altered fibrin-network formation. The kinetics by which FXIII is activated has indeed been reported to have an important effect on the final structure of the fibrin network. For instance, the Val34Leu polymorphism in FXIII is associated with accelerated activation by thrombin, and results in a fibrin meshwork with thinner fibers and reduced porosity.[31,32]

It should be noted that discordant data have been described with regard to the formation of the fibrin network in the presence of emicizumab. Shimonishi *et al*. reported that the aPTT-reagent triggered fibrin-network generated *in vitro* in the presence of emicizumab was similar to that of FVIII-induced fibrin.[16] In contrast, Janbain *et al.* found that fibrin-fibers produced in the presence of emicizumab were almost 2-fold thinner than those produced in the presence of FVIII at a concentration of 10 IU/dl.[17,33] When comparing the protocols to obtain scanning-EM images to analyze the fibrin-structure, it appears that each of these studies used a different protocol for dehydration. Differences in dehydration-protocols may affect how fibers are represented within scanning-EM images. Second, artificial activating reagents were used in the *in vitro* studies by Shimonishi *et al.* and Janbain *et al.*, whereas the fibrin structures in our study were obtained from *in vivo* generated clots, a more physiological environment that also contains other blood components (red blood cells, platelets). Each of these blood components contribute to the formation of the fibrin-network and its ultimate structure.[34]

Consequences of different clot architecture: It is tempting to speculate that the unstable clots originate from a modified fibrin-network. Although no direct evidence is provided in this study, the presented *in vivo* data are compatible with this scenario. In particular, a dense fibrin structure may modify the biomechanical properties of the clot, and the unusual thick fibers may reduce its elasticity.[35] Such increased rigidity seems in keeping with the rebleeds that are observed upon clot removal in emicizumab-treated mice, but not rFVIII- or rFVIIIFc-treated mice (Figure 2).

In conclusion, rFVIII and rFVIIIFc act similarly regarding clot formation and structure. In contrast, the different mode of action of emicizumab alters the kinetics of fibrin and FXIIIa formation, resulting in different clot morphologies. We are aware that these data represent only part of the differences that may occur in FVIII- *versus* emicizumab-dependent clot formation. Additional studies are in progress aiming to expand our notion of how non-factor molecules like emicizumab modify the clot architecture and therefore the hemostatic process.

References

1. Versteeg HH, Heemskerk JW, Levi M, Reitsma PH. New fundamentals in hemostasis. Physiol Rev. 2013;93(1):327-358.
2. Wolberg AS, Sang Y. Fibrinogen and Factor XIII in Venous Thrombosis and Thrombus Stability. Arterioscler Thromb Vasc Biol. 2022;42(8):931-941.
3. Sillen M, Declerck PJ. Thrombin Activatable Fibrinolysis Inhibitor (TAFI): An Updated Narrative Review. Int J Mol Sci. 2021;22(7):3670.
4. Domingues MM, Macrae FL, Duval C, et al. Thrombin and fibrinogen gamma' impact clot structure by marked effects on intrafibrillar structure and protofibril packing. Blood. 2016;127(4):487-495.
5. Lenting PJ, van Mourik JA, Mertens K. The life cycle of coagulation factor VIII in view of its structure and function. Blood. 1998;92(11):3983-3996.
6. Mancuso ME, Mahlangu JN, Pipe SW. The changing treatment landscape in haemophilia: from standard half-life clotting factor concentrates to gene editing. Lancet. 2021;397(10274):630-640.
7. Sankar AD, Weyand AC, Pipe SW. The evolution of recombinant factor replacement for hemophilia. Transfus Apher Sci. 2019;58(5):596-600.
8. Weyand AC, Pipe SW. New therapies for hemophilia. Blood. 2019;133(5):389-398.
9. Oldenburg J, Mahlangu JN, Kim B, et al. Emicizumab Prophylaxis in Hemophilia A with Inhibitors. N Engl J Med. 2017;377(9):809-818.
10. Mahlangu J, Oldenburg J, Paz-Priel I, et al. Emicizumab Prophylaxis in Patients Who Have Hemophilia A without Inhibitors. N Engl J Med. 2018;379(9):811-822.
11. Callaghan MU, Negrier C, Paz-Priel I, et al. Long-term outcomes with emicizumab prophylaxis for hemophilia A with or without FVIII inhibitors from the HAVEN 1-4 studies. Blood. 2021;137(16):2231-2242.
12. Mahlangu J, Iorio A, Kenet G. Emicizumab state-of-the-art update. Haemophilia. 2022;28 Suppl 4(Suppl 4):103-110.
13. Batsuli G, Wheeler AP, Weyand AC, Sidonio RFJr., Young G. Severe muscle bleeds in children and young adults with hemophilia A on emicizumab prophylaxis: Real-world retrospective multi-institutional cohort. Am J Hematol. 2023;98(10):E285-E287.
14. Lenting PJ, Denis CV, Christophe OD. Emicizumab, a bispecific antibody recognizing coagulation factors IX and X: how does it actually compare to factor VIII? Blood. 2017;130(23):2463-2468.
15. Zong Y, Antovic A, Soutari NMH, Antovic J, Pruner I. Synergistic Effect of Bypassing Agents and Sequence Identical Analogue of Emicizumab and Fibrin Clot Structure in the In Vitro Model of Hemophilia A. TH Open. 2020;4(2):e94-e103.

16. Shimonishi N, Nogami K, Ogiwara K, et al. Emicizumab improves the stability and structure of fibrin clot derived from factor VIII-deficient plasma, similar to the addition of factor VIII. Haemophilia. 2020;26(3):e97-e105.
17. Janbain M, Enjolras N, Bolbos R, Brevet M, Bordet JC, Dargaud Y. Haemostatic effect of adding tranexamic acid to emicizumab prophylaxis in severe haemophilia A: A preclinical study. Haemophilia. 2021;27(6):1002-1006.
18. Schultz NH, Glosli H, Bjornsen S, Holme PA. The effect of emicizumab and bypassing agents in patients with hemophilia - An in vitro study. Res Pract Thromb Haemost. 2021;5(5):e12561.
19. Bravo MI, Raventos A, Perez A, Costa M, Willis T. Non-additive effect on thrombin generation when a plasma-derived factor VIII/von Willebrand factor (FVIII/VWF) is combined with emicizumab in vitro. J Thromb Haemost. 2020;18(8):1934-1939.
20. Dargaud Y, Lienhart A, Janbain M, Le Quellec S, Enjolras N, Negrier C. Use of thrombin generation assay to personalize treatment of breakthrough bleeds in a patient with hemophilia and inhibitors receiving prophylaxis with emicizumab. Haematologica. 2018;103(4):e181-e183.
21. Kizilocak H, Marquez-Casas E, Phei Wee C, Malvar J, Carmona R, Young G. Comparison of bypassing agents in patients on emicizumab using global hemostasis assays. Haemophilia. 2021;27(1):164-172.
22. Atsou S, Schellenberg C, Lagrange J, et al. Thrombin generation on vascular cells in the presence of factor VIII and/or emicizumab. J Thromb Haemost. 2023 Sep 29. [Epub ahead of print]
23. Ferriere S, Peyron I, Christophe OD, et al. A hemophilia A mouse model for the in vivo assessment of emicizumab function. Blood. 2020;136(6):740-748.
24. Johansen PB, Tranholm M, Haaning J, Knudsen T. Development of a tail vein transection bleeding model in fully anaesthetized haemophilia A mice - characterization of two novel FVIII molecules. Haemophilia. 2016;22(4):625-631.
25. Rawle FE, Lillicrap D. Preclinical animal models for hemophilia gene therapy: predictive value and limitations. Semin Thromb Hemost. 2004;30(2):205-213.
26. Lozier JN, Nichols TC. Animal models of hemophilia and related bleeding disorders. Semin Hematol. 2013;50(2):175-184.
27. Locke M, Receveur N, Kiialainen A, David T. In vitro investigation of emicizumab efficacy and mode of action in vWD type 2 and 3 samples. Res Pract Thromb Haemost. 2022;6(S1):630.
28. Adamkewicz JI, Chen DC, Paz-Priel I. Effects and Interferences of Emicizumab, a Humanised Bispecific Antibody Mimicking Activated Factor VIII Cofactor Function, on Coagulation Assays. Thromb Haemost. 2019;119(7):1084-1093.

29. Antovic A, Mikovic D, Elezovic I, Zabczyk M, Hutenby K, Antovic JP. Improvement of fibrin clot structure after factor VIII injection in haemophilia A patients treated on demand. Thromb Haemost. 2014;111(4):656-661.
30. Wolberg AS, Allen GA, Monroe DM, Hedner U, Roberts HR, Hoffman M. High dose factor VIIa improves clot structure and stability in a model of haemophilia B. Br J Haematol. 2005;131(5):645-655.
31. Ariens RA, Philippou H, Nagaswami C, Weisel JW, Lane DA, Grant PJ. The factor XIII V34L polymorphism accelerates thrombin activation of factor XIII and affects cross-linked fibrin structure. Blood. 2000;96(3):988-995.
32. Kattula S, Bagoly Z, Toth NK, Muszbek L, Wolberg AS. The factor XIII-A Val34Leu polymorphism decreases whole blood clot mass at high fibrinogen concentrations. J Thromb Haemost. 2020;18(4):885-894.
33. Janbain M, Enjolras N, Bordet JC, et al. Hemostatic effect of tranexamic acid combined with factor VIII concentrate in prophylactic setting in severe hemophilia A: A preclinical study. J Thromb Haemost. 2020;18(3):584-592.
34. Leong L, Chernysh IN, Xu Y, et al. Clot stability as a determinant of effective factor VIII replacement in hemophilia A. Res Pract Thromb Haemost. 2017;1(2):231-241.
35. Feller T, Connell SDA, Ariëns RAS. Why fibrin biomechanical properties matter for hemostasis and thrombosis. J Thromb Haemost. 2022;20(1):6-16.

Legends

Figure 1: Incomplete wound closure.

Hemophilic patient on emicizumab prophylaxis arrived in the hospital with a deep laceration in his foot (day 1). The wound was treated with local tranexamic acid application and covered with steri-strips. At day 10, steri-strips were removed, but the wound was still open, and no wound closure or healing was observed. Patient received FVIII treatment on days 10 and 11. At day 12, wound closure was observed and wound healing process progressed gradually during the following days (day 13 & day 16).

Figure 2: Hemostatic responses after tail vein-transection without and with clot removal.

At a tail-diameter of 2.3mm, an incision with a depth of 0.5mm in the left lateral vein was made. Mice receiving emicizumab also received human FIX and human FX (both 100 IU/kg) 5 min before injury. Both panels depict the bleeding profile of mice receiving vehicle, rFVIII, rFVIIIFc or emicizumab. Plasma concentrations at the start of the procedure were 10 IU/dl for rFVIII and rFVIIIFc and 55 μg/ml for emicizumab. Black represents period of bleeding, grey periods of minor bleeding, and white periods of non-bleeding. *A:* The wound remained unchallenged after the transection of the vein. *B:* Dotted lines at 900 seconds and 1800 seconds indicate timing of clot removal in mice that did not bleed at those instants. Emicizumab + FIX/FX 12' refers to re-injection of FIX and FX at t=12 min in emicizumab-treated mice, *ie.* 3 min before the first clot removal. Emicizumab + TXA refers to emicizumab-treated mice that also received tranexamic acid (10 mg/kg) 5 min before injury. Amounts of blood loss measured in these mice are presented in supplementary figure S1.

Figure 3: *In vitro* fibrin formation and fibrinolysis. *Panel A:* Schematic representation of *in vitro* fibrin formation in human FVIII-deficient plasma supplemented with rFVIII or emicizumab. *Panels B-E:* FVIII-deficient plasma (*panel B*) was supplemented with rFVIII at 10 IU/dl (*C*) or 100 IU/dl (*D*) or emicizumab at 55 μg/ml (*E*). In addition, fibrinogen was added (1 mg/ml final concentration) and the reaction was initiated by the addition of $CaCl_2$. No other additives (tissue factor or factor XIa) were used. Fibrin formation was detected by monitoring OD-values at 405nm, while FXIII activity was measured via hydrolysis of the fluorescent A101 substrate (excitation 313 nm; emission 418 nm). Red line: fibrin formation (left Y-axis) and blue line: FXIII activity (right Y-axis). Presented are the mean (solid lines) and standard error (grey area around the solid line) of 6-8 measurements. AFU: arbitrary fluorescence units.

Figure 4: Scanning-EM imaging of *in vivo* generated fibrin networks. *Panel A:* experimental approach for the preparation of tissue sections. The black rectangle indicates the region examined using scanning-EM. *Panels B-C:* Tail fragments obtained 10 min after TVT were prepared for scanning-EM using standard pre-fixation with 4% glutaraldehyde and 1% OsO4 and dehydration. Presented are representative images of FVIII-deficient mice treated with rFVIII (*panel B*), or emicizumab (*panel C*). Plasma concentrations at the start of the procedure were 10 IU/dl for rFVIII and 55 μg/ml for emicizumab. Scale bars represent 10 microns in the large image, and 5 microns in the amplified images. White boxes indicate regions of numeric zooms. *Panels D-G:* ImageJ-plugin software was used to determine fibrin coverage (% *per* field; *panel D*), average fibrin diameter (in micron *per* field; *panel E*), number of pores *per* field (*panel F*) and the number of intersections *per* field (panel *G*). For each graph, 2 mice were included (round and triangle symbols) and 10 fields *per* mouse were examined. Each symbol represents the result of a single field. Statistical analysis was performed using unpaired Student's t-test.

Figure 5: Fibrin content within the injured area. *Panel A:* experimental approach for the preparation of tissue sections. The black rectangle indicates the region examined using spinning disk confocal imaging. *Panels B-F:* Tail tissue sections obtained 10 min after TVT were prepared for immunofluorescence staining using an anti-mouse fibrin antibody. *Panels B-F:* representative images of wild-type (WT)-mice (*panel B*), untreated FVIII-deficient mice (FVIII-KO; *panel C*); FVIII-deficient mice treated with rFVIII (*panel D_1-D_2*), rFVIIIFc (*panel E_1-E_2*), or emicizumab (*panel F_1-F_2*). Plasma concentrations at the start of the procedure were 10 IU/dl for rFVIII and rFVIIIFc and 55 μg/ml for emicizumab. *Panel G:* For each condition, two non-subsequent tissue sections of five mice (represented by square, round, diamond, up-triangle and down-triangle symbols) were analyzed using ImageJ-software for the fluorescence intensity (*panel E*). Statistical analysis was performed using one-way ANOVA with Tukey's corrections for multiple comparisons. Only statistically significant differences ($p<0.05$) are indicated. Each symbol represents a separate tissue section of an individual mice, and mean±SD are indicated for each condition.

Figure 6: Fibrin structures imaged using stimulated emission depletion (STED)-microscopy. *Panel A:* experimental approach for the preparation of tissue sections. The black rectangle indicates the region examined using STED-microscopy. *Panels B-E*: Representative images of wild-type mice (WT; *panel B),* FVIII-deficient mice treated with rFVIIIFc (*panels C_1-C_3*), untreated FVIII-deficient mice (FVIII-KO; *panel D*) or FVIII-deficient mice treated with emicizumab (*panels E_1-E_3*). Fibrin was detected using polyclonal goat anti-murine fibrin antibodies, and probed using STAR-RED-labeled donkey anti-goat antibodies.

Plasma concentrations at the start of the procedure were 10 IU/dl for rFVIIIFc and 55 μg/ml for emicizumab. *Panel F:* For each condition, 30 images from 3 different mice (10/mouse) were analyzed using ImageJ-software to calculate the presence of dot-like structures. White arrows in panels C_1-C_3 indicate examples of dot-like structures. Statistical analysis was performed using One-way ANOVA with Dunnet's test for multiple comparisons.

Figure 7: Correlation between *in vitro* and *in vivo* fibrin generation. *Panel A:* The amount of fibrin generated (referred to as fibrin coverage) *in vivo* under different conditions (data presented in figure 4 and Supplementary figure S3) was plotted against the *in vitro* amount of fibrin generated (referred to as maximal (max) absorbance; data presented in figure 3). *Panel B:* The amount of fibrin generated (referred to as mean fluorescence intensity; MFI) *in vivo* under different conditions (data presented in figure 5) was plotted against the *in vitro* amount of fibrin generated (referred to as maximal (max) absorbance; data presented in figure 3).
Red symbol: FVIII-KO mice vs FVIII-deficient plasma; orange symbol: FVIII-KO mice receiving 10 IU/dl rFVIII versus FVIII-deficient plasma spiked with 10 IU/dl rFVIII; Green symbol: wild-type (WT)-mice versus FVIII-deficient plasma spiked with 100 IU/dl rFVIII; Blue symbol: FVIII-KO mice receiving emicizumab (55 μg/ml) versus FVIII-deficient plasma spiked with emicizumab (55 μg/ml).

A: day 1

B: day 10

C: day 12

D: day 13

E: day 16

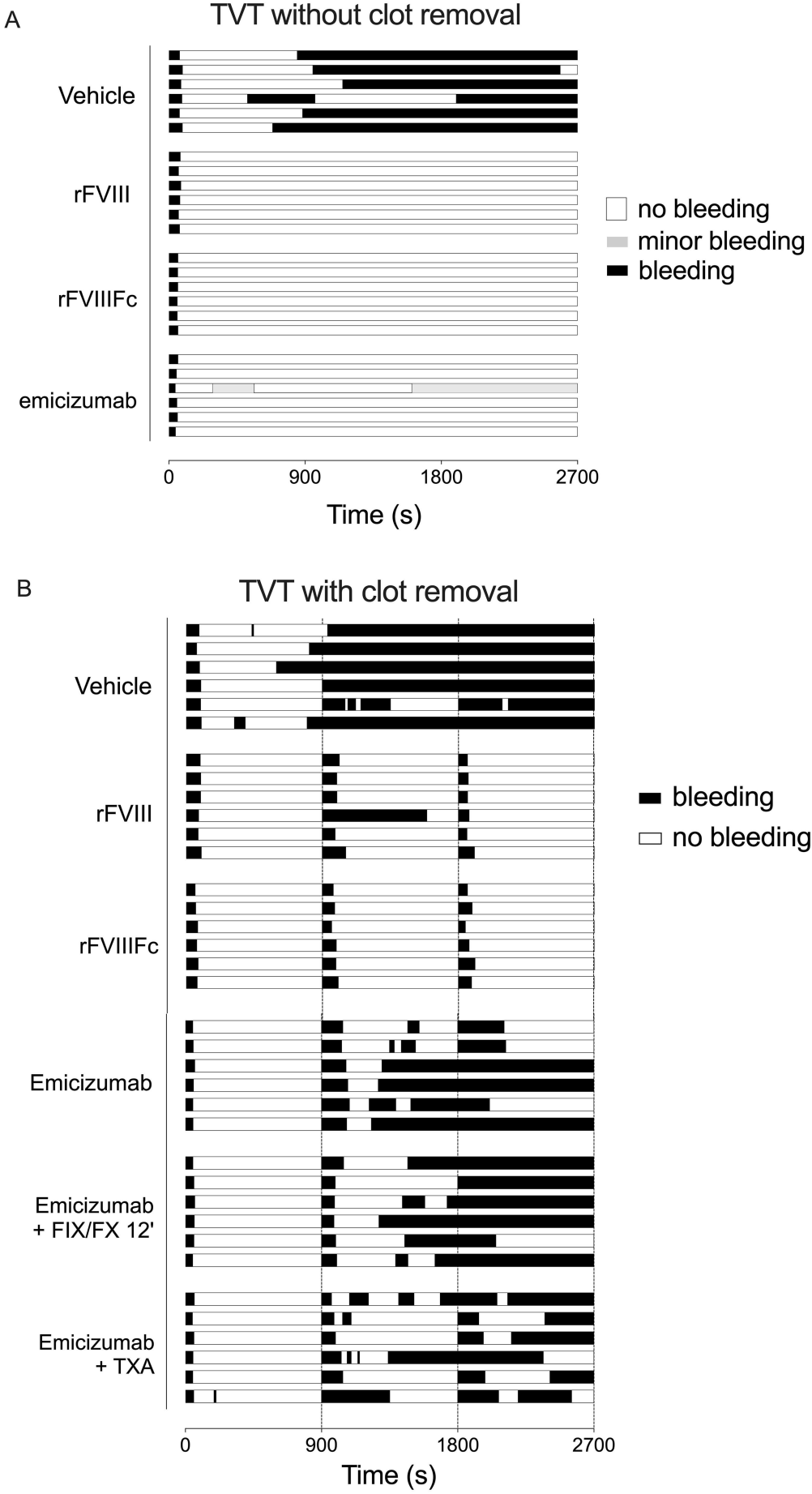
A
TVT without clot removal
Vehicle
rFVIII
rFVIIIFc
emicizumab
no bleeding
minor bleeding
bleeding
0
900
1800
2700
Time (s)
B
TVT with clot removal
Vehicle
rFVIII
rFVIIIFc
Emicizumab
Emicizumab
+ FIX/FX 12'
Emicizumab
+ TXA
bleeding
no bleeding
0
900
1800
2700
Time (s)

Figure 3

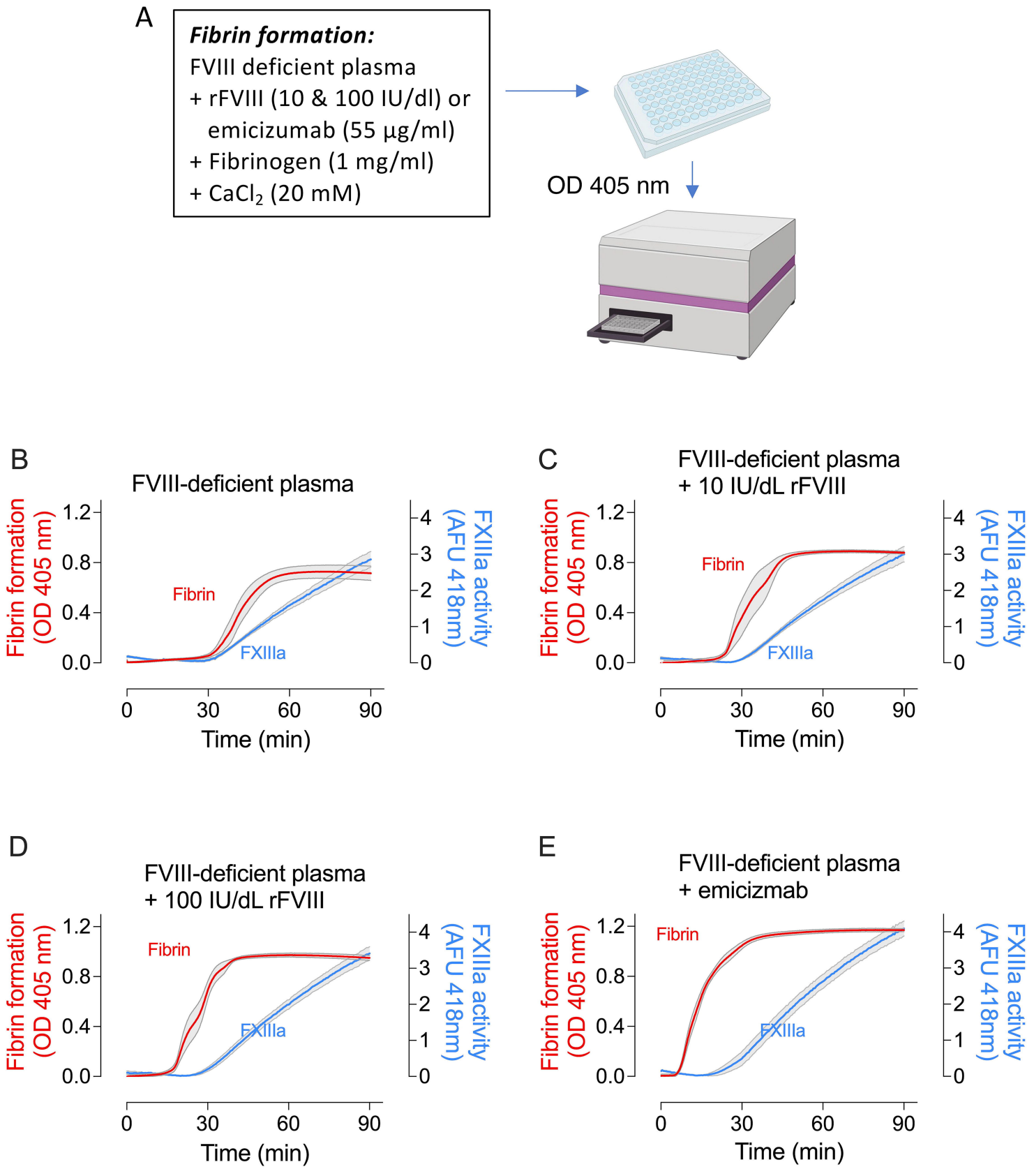
A
Fibrin formation:
FVIII deficient plasma
+ rFVIII (10 & 100 IU/dl) or
emicizumab (55 µg/ml)
+ Fibrinogen (1 mg/ml)
+ CaCl2 (20 mM)
OD 405 nm
B
FVIII-deficient plasma
C
FVIII-deficient plasma
+ 10 IU/dL rFVIII
D
FVIII-deficient plasma
+ 100 IU/dL rFVIII
E
FVIII-deficient plasma
+ emicizmab
Fibrin formation (OD 405 nm)
FXIIIa activity (AFU 418nm)
Fibrin
FXIIIa
Time (min)
0
30
60
90
0.0
0.4
0.8
1.2
0
1
2
3
4

Figure 4

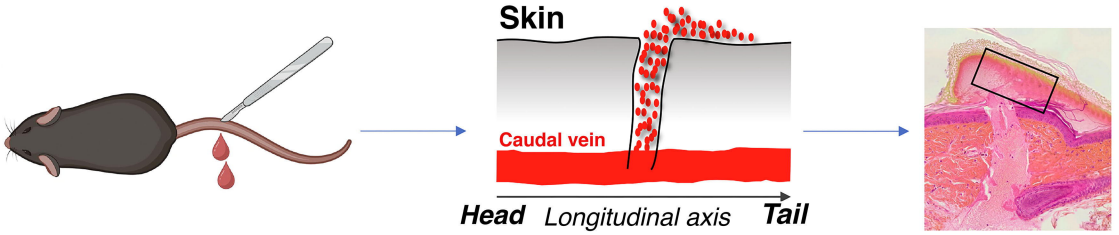
Skin
Caudal vein
Head
Longitudinal axis
Tail

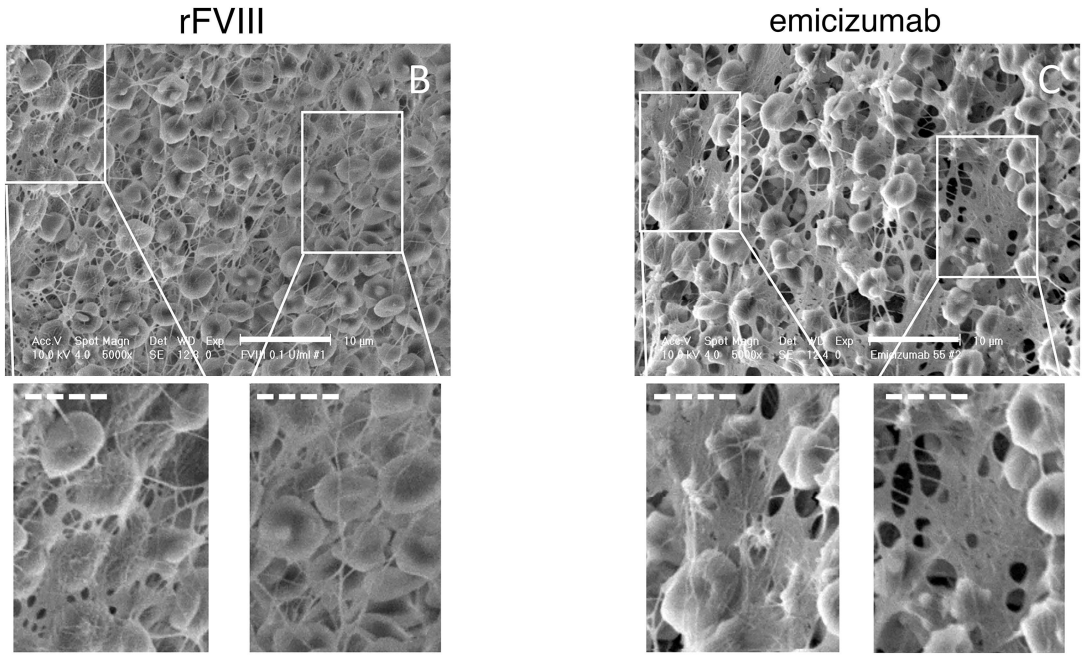
rFVIII
emicizumab
B
C

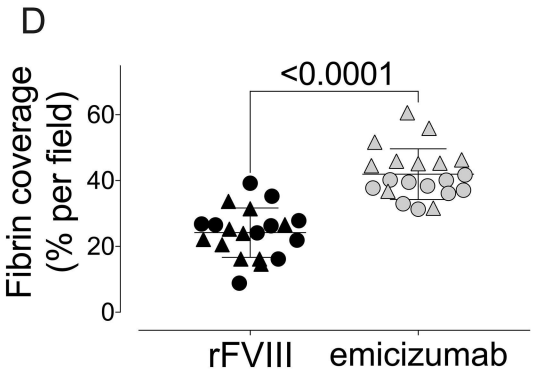
D
Fibrin coverage (% per field)
<0.0001
rFVIII
emicizumab

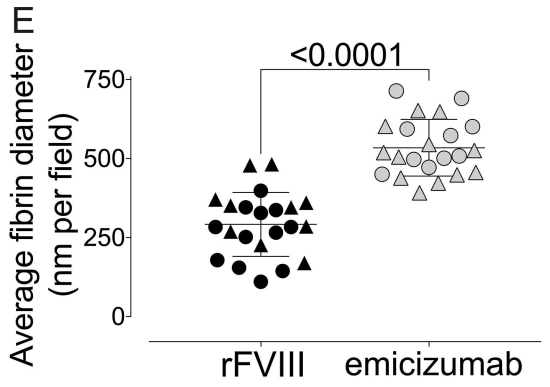
E
Average fibrin diameter (nm per field)
<0.0001
rFVIII
emicizumab

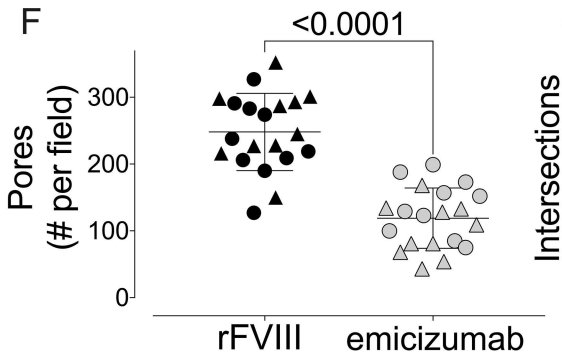
F
Pores (# per field)
<0.0001
rFVIII
emicizumab

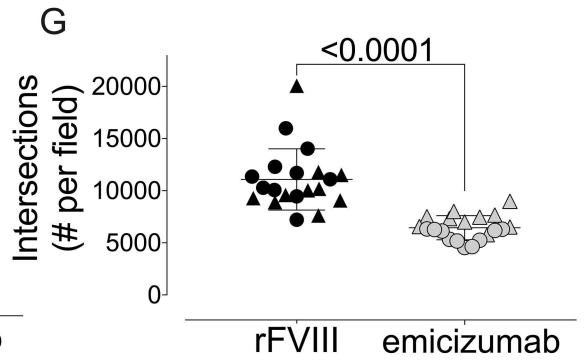
G
Intersections (# per field)
<0.0001
rFVIII
emicizumab

Figure 5

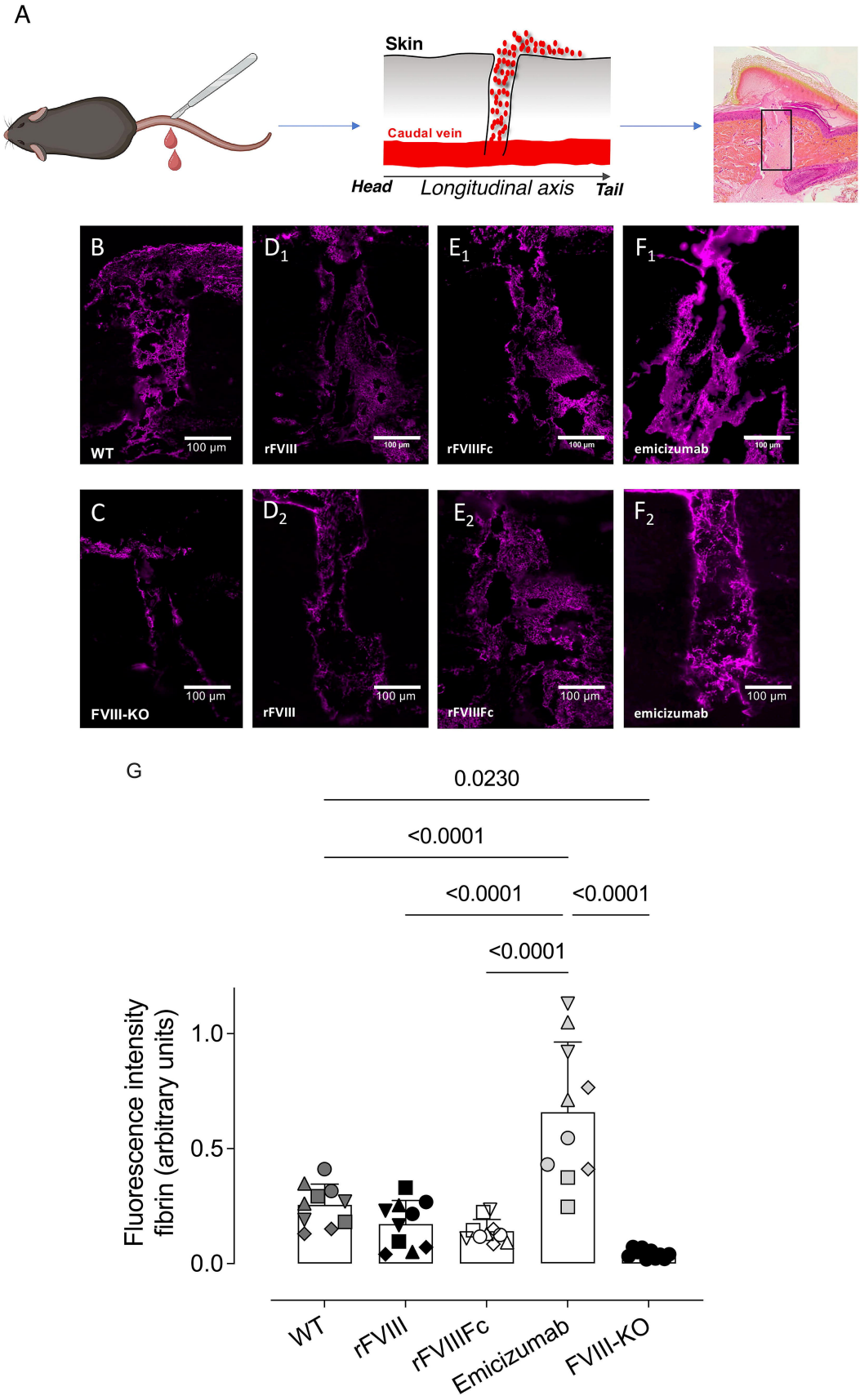
A
Skin
Caudal vein
Head
Longitudinal axis
Tail
B
WT
100 µm
D1
rFVIII
E1
rFVIIIFc
F1
emicizumab
C
FVIII-KO
D2
rFVIII
E2
rFVIIIFc
F2
emicizumab
G
0.0230
<0.0001
<0.0001
<0.0001
<0.0001
Fluorescence intensity
fibrin (arbitrary units)
1.0
0.5
0.0
WT
rFVIII
rFVIIIFc
Emicizumab
FVIII-KO

Figure 6

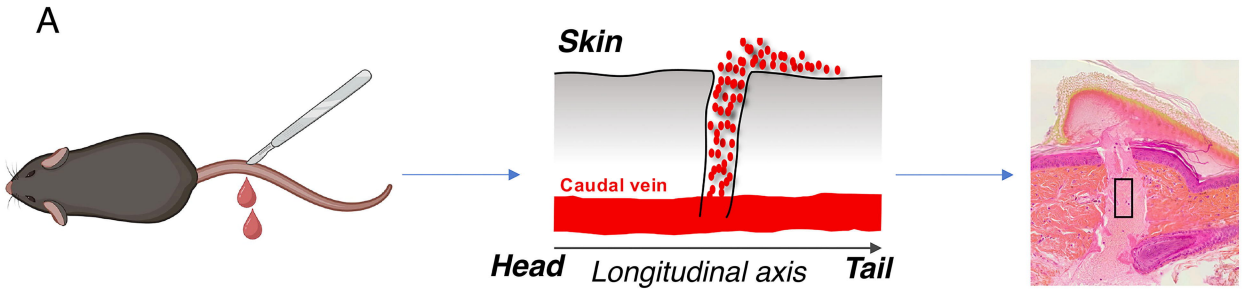
A
Skin
Caudal vein
Head
Longitudinal axis
Tail

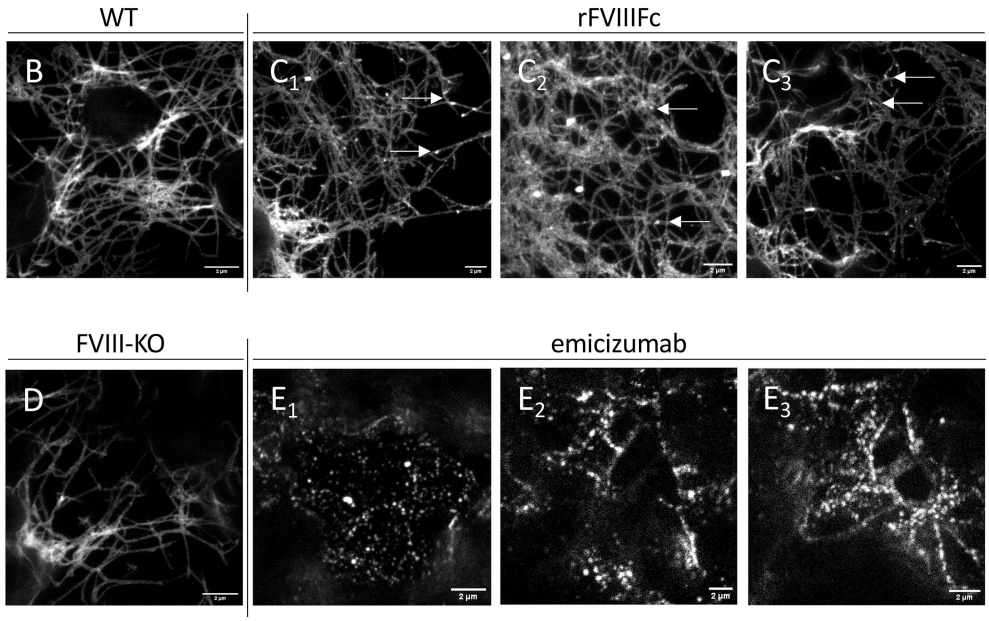
WT
rFVIIIFc
B
C1
C2
C3
FVIII-KO
emicizumab
D
E1
E2
E3

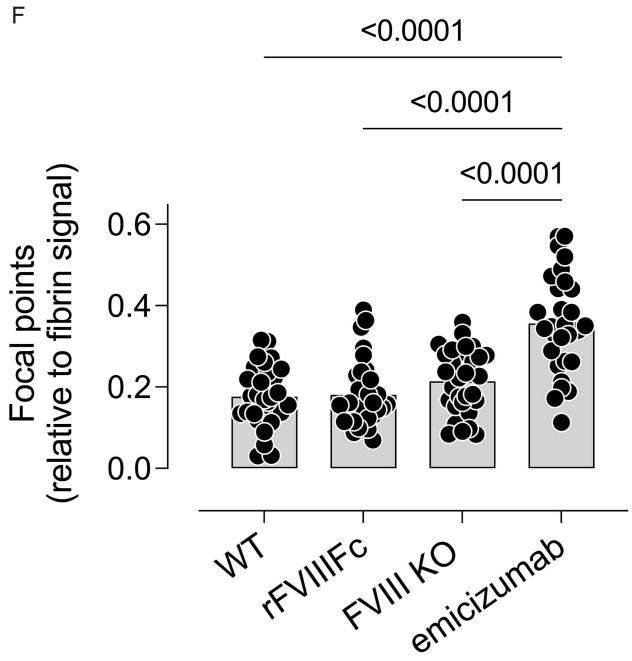
F
<0.0001
<0.0001
<0.0001
Focal points
(relative to fibrin signal)
0.6
0.4
0.2
0.0
WT
rFVIIIFc
FVIII KO
emicizumab

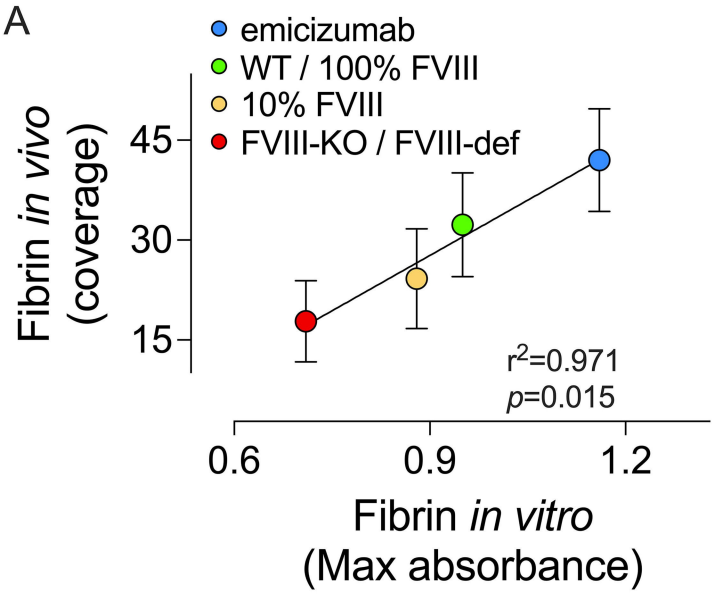
A
emicizumab
WT / 100% FVIII
10% FVIII
FVIII-KO / FVIII-def
Fibrin *in vivo*
(coverage)
45
30
15
r²=0.971
p=0.015
0.6
0.9
1.2
Fibrin *in vitro*
(Max absorbance)

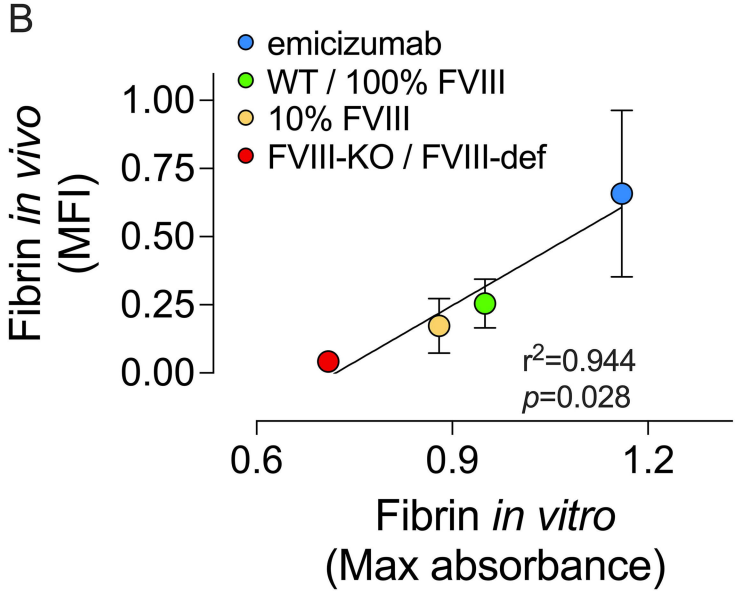
B
emicizumab
WT / 100% FVIII
10% FVIII
FVIII-KO / FVIII-def
Fibrin *in vivo*
(MFI)
1.00
0.75
0.50
0.25
0.00
r²=0.944
p=0.028
0.6
0.9
1.2
Fibrin *in vitro*
(Max absorbance)

Supplementary materials

Differences in venous clot structures between hemophilic mice treated with emicizumab versus factor VIII or factor VIIIFc

Thibaud Sefiane et al.

Supplementary methods

Animals and ethics statement

F8-deficient mice[1] were backcrossed (>10 times) on a C57Bl/6 background. Males and females were used throughout the study (8-12 weeks old, 20-25 g). Housing and experiments were performed in accordance with French regulations and the experimental guidelines of the European Community. This project was approved by the local ethical committee of Université Paris-Saclay (Comité d'Ethique en Experimentation Animale n°26, protocol APAFIS#26510-202007061525281 v2).

Patient information

A 2-year-old boy with severe haemophilia A (FVIII <1%) on regular prophylaxis with emicizumab (6 mg/kg every 4 weeks, subcutaneously) since the age of 8 months (*per* policy of the local treatment center). The patient had no relevant bleeding history and has no history of FVIII inhibitors. He experienced a first small muscle bleed after intramuscular vaccination at the age of 2 months, which was treated with standard half-life rFVIII. A second bleed at the age of 5 months due to an injury of his finger, was also treated with standard half-life rFVIII. The patient has no comorbidities or other chronic treatment besides emicizumab. While on emicizumab, the patient had zero treated bleeds, but reported three non-treated bleeds (post-traumatic haematoma, small wound and dentition, for the latter of which the patient received additional tranexamic acid). The incidence described in this study concerns a glass-induced deep laceration at his left foot.

Proteins & materials

Emicizumab (marketed under Hemlibra) was from F. Hoffman-La Roche (Basel, Switzerland). Recombinant factor IX (FIX, Benefix) was from Pfizer (Paris, France). Plasma-derived factor X (FX) was from Cryopep (Montpellier, France). Recombinant factor VIII (rFVIII, Advate) was from Shire France SAS (Paris, France). Recombinant FVIIIFc (rFVIIIFc, Elocta) was from Sobi (Stockholm, Sweden). Tranexamic acid was from Mylan (Paris, France), and generously provided by Dr. Dominique Lasne. DAPI and Alexafluor 647-labeled chicken anti-goat antibodies were from Invitrogen (Saint Aubin, France). Polyclonal rabbit anti-human Fc was from Synobiological (Düsseldorf, Germany). Polyclonal goat anti-mouse fibrin antibodies (cat#

YNGMFBG7S) were from Accurate chemical (Carle Place, NY). Although categorized as anti-murine fibrinogen antibodies, these antibodies recognize fibrin and cross-linked fibrin but not murine fibrinogen in Elisa and tissue sections. STAR RED-labeled donkey anti goat antibodies used for Stimulated Emission Depletion (STED)-microscopy were from Abberior (Göttingen, Germany). FVIII-deficient plasma and purified fibrinogen (depleted for VWF and fibrin) were from Stago BNL (Leiden, the Netherlands). Fluorescent substrate A101 for FXIIIa was from Interchim (Montluçon, France).

Emicizumab-compatible mouse model

Mice were given emicizumab via retro-orbital intravenous injection 24 h before tail vein-transection (TVT) to obtain plasma concentrations of 55 μg/ml at the time of the transection.[2] A second retro-orbital injection was given 5 min before the TVT-procedure, using a solution containing human FIX and FX (both 100 U/kg).

FVIII-mediated correction of bleeding

Mice were given rFVIII or rFVIIIFc (100 μl volume) via retro-orbital injection 5 min before TVT to obtain plasma concentrations of 10 IU/dl at the time of the transection.

Tail vein-transection

For the tail vein-transection (TVT)-procedure, mice were anesthetized with isoflurane and a precise cut of the caudal tail vein was performed as described.[3] After vein transection, the tail was immediately immersed in physiological saline, prewarmed at 37 °C. At the end of the assay (45 min observation time) animals were sacrificed by cervical dislocation. Mean values of the blood loss volume (μl) were reported. The mixture of collected blood and physiological saline was centrifuged at 1,500 *g*. The red blood cell pellet was then lysed in H_2O and the amount of hemoglobin was determined by reading the absorbance at 416 nm. The volume of blood loss in each sample was calculated from a standard curve, which was obtained by lysing defined volumes of mouse blood (20-40-60-80-100 μl) in H_2O to extract hemoglobin.

Fibrin formation

Fibrin formation experiments were performed in half-well microtiter-plates in a volume of 100 μl. Mixtures consisted of FVIII-deficient plasma (50 μl), purified fibrinogen (40 μl of 2.5 mg/ml), and rFVIII, rFVIIIFc or emicizumab (5 μl of 200 IU/dl to reach 10 IU/dl rFVIII or rFVIIIFc; 5 μl of 2000 IU/dl to reach 100 IU/dl rFVIII or rFVIIIFc: 5 μl of 1.1 mg/ml to reach 55 μg/ml emicizumab). The reaction was started by the addition of $CaCl_2$ (5 μl/well). OD at 405 nm was measured every 30 sec for a 2 h period.

FXIIIa generation

FXIIIa generation experiments were performed in half-well microtiter-plates in a volume of 100 µl. Mixtures consisted of FVIII-deficient plasma (50 µl), purified fibrinogen (40 µl of 2.5 mg/ml), and rFVIII, rFVIIIFc or emicizumab (5 µl of 200 IU/dl to reach 10 IU/dl rFVIII or rFVIIIFc; 5 µl of 2000 IU/dl to reach 100 IU/dl rFVIII or rFVIIIFc: 5 µl of 1.1 mg/ml to reach 55 µg/ml emicizumab). The reaction was started by the addition of $CaCl_2$ (5 µl/well). FXIIIa generation was monitored using fluorescent substrate A101 (excitation 313 nm; emission 418 nm).

Scanning electron microscopy

Dehydration-preparation: 10 min after the TVT-procedure, the whole tail was dissected and immediately immerged in 4% PFA/1% glutaraldehyde and fixed overnight at 4 °C. Preparation of the sections for analysis was performed essentially as described.[4] A 1-cm tail section centered around the injury was progressively dehydrated via serial alcohol incubations: 2x 10 min in 50% ethanol, 2x 10 min in 70% ethanol, 2x 10 min in 95% ethanol, 3x 15 min in 100% ethanol. All incubation were performed under gentle agitation. Dehydrated sections were dried using hexamethyldisilazane (HMDS) as follows: 15 min in 2:1 100% ethanol/HMDS, 15 min in 1:1 100% ethanol/HMDS, 15 min in 1:2 100% ethanol/HMDS and 3x 15 min in HMDS. Samples were metallized using a sputtering device (Balzers Sputter Coater SCD 050; Leica) with the following setting: 10 nm of silver; 120 seconds at 5 cm; 30 mA.

Samples were immediately analyzed using a Philips XL-Environmental Scanning Electron Microscope.

Immunostaining of fibrin

The whole tail was dissected 10 min after the TVT-procedure, immediately immerged in 4% paraformaldehyde (PFA), and fixed overnight at 4 °C. A 1-cm tail section centered around the injury was prepared and washed for 2h in PBS and embedded in Tissue-Tek optimum-cutting temperature (OCT)-compound. Tissues sections of 7 µm were collected using a cryostat (Leica) on glass slides. Staining of fibrin was performed using polyclonal goat antibodies against murine fibrin/fibrinogen (6 µg/ml) and Alexafluor 647-labeled chicken anti-goat antibodies (4 µg/ml). Images were obtained using high-resolution tilling reconstruction using spinning disk confocal microscopy (Olympus IX73 equipped with CrestOptics X-Light V1) as described previously.[5] Quantification of immunofluorescence was performed using ImageJ-software.

Stimulated Emission Depletion (STED)-microscopy

Tissues sections were generated and stained for fibrin as described under “Immunostaining for fibrin”, with the exception that STAR RED-labeled donkey anti goat antibodies (5 µg/ml) were used as secondary antibody. STED microscopy was performed on the Stedycon system (Abberior Instruments, Göttingen, Germany) composed of an AxioObserver 7 inverted microscope (Zeiss, Germany).[6]

Image analysis

Image analysis was performed using ImageJ-software. DiameterJ-plugin was used for the analysis of the Scanning-EM images of the fibrin-network.

Statistical analysis

All data are presented as mean±standard deviation (mean±SD) unless indicated otherwise. Number (*n*) refer to the number of independent experiments or animals. The statistical analysis was performed using GraphPad Prism 9 software for Mac (La Jolla, California, USA). One-way analysis of variance (1-way ANOVA) followed by Tukey’s or Dunnett’s multiple comparison test was performed when comparing multiple groups. Pairwise analysis was performed using the unpaired Student’s t-test or the Mann-Whitney test, where appropriate. $P<0.05$ was considered as statistically significant.

Supplementary figure S1

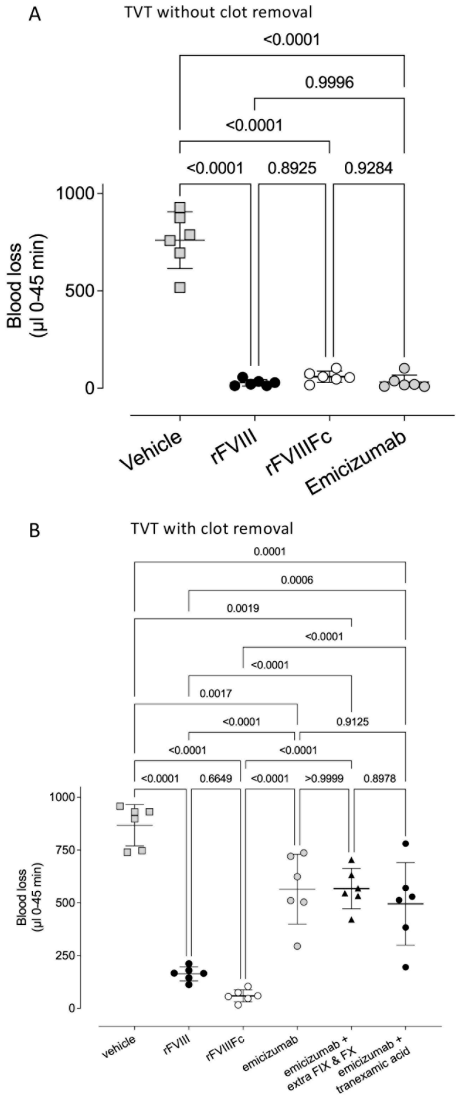

Supplementary figure S1: Blood loss in FVIII-deficient mice after treatment with rFVIII, rFVIIIFc or emicizumab.

At a tail-diameter of 2.3 mm, an incision with a depth of 0.5 mm in the left lateral vein was made, and blood loss was monitored for 45 min. Mice were given emicizumab 24 h before injury, allowing plasma concentrations of 55 μg/ml at the start of the TVT-procedure. In addition, mice received human factor IX and factor X (both 100 IU/kg) 5 min before injury. Concentrations of rFVIII and rFVIIIFc were 10 IU/dl at the time of injury. *Panel A:* Blood loss in mice without clot removal. *Panel B:* At 15 min and 30 min after injury, the clot was removed via gentle wiping, but only if the mouse was not bleeding at that particular moment. One series of mice (Emicizumab + extra FIX & FX) received additional FIX/FX at a dose of 100 IU/kg at 12 min after injury, *ie.* 3 min before the first clot removal. A second series of mice (Emicizumab + tranexamic acid) received tranexamic acid at a dose of 10 mg/kg at 5 min before injury. Statistical analysis was performed via One-way ANOVA with Tukey's correction for multiple comparisons.

Supplementary figure S2

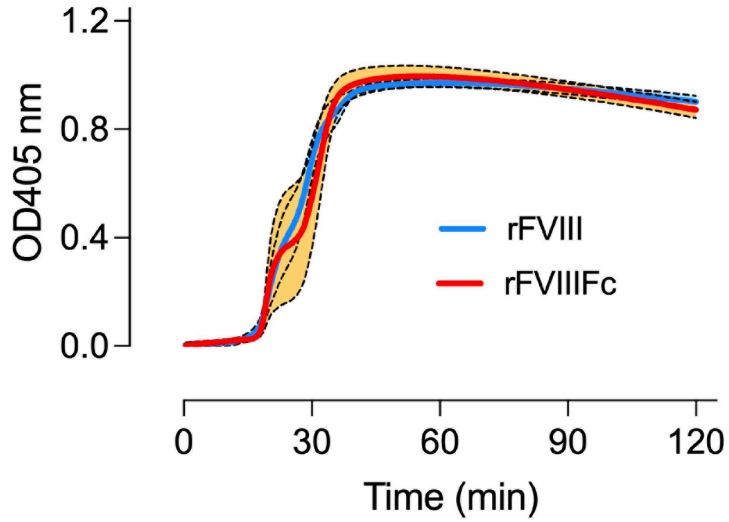

Legend Supplementary figure S2: In vitro fibrin formation comparing rFVIII to rFVIIIFc. FVIII-deficient plasma was supplemented with rFVIII or rFVIIIFc at 100 IU/dl. In addition, fibrinogen was added (1 mg/ml final concentration) and the reaction was initiated by the addition of $CaCl_2$. No other additives (tissue factor or factor XIa) were used. Fibrin formation was detected by monitoring OD-values at 405 nm. Blue line: rFVIII and red line: rFVIIIFc. Presented are the mean (solid lines) and standard error (orange-colored areas around the solid line) of 6-8 measurements.

Supplementary figure S3

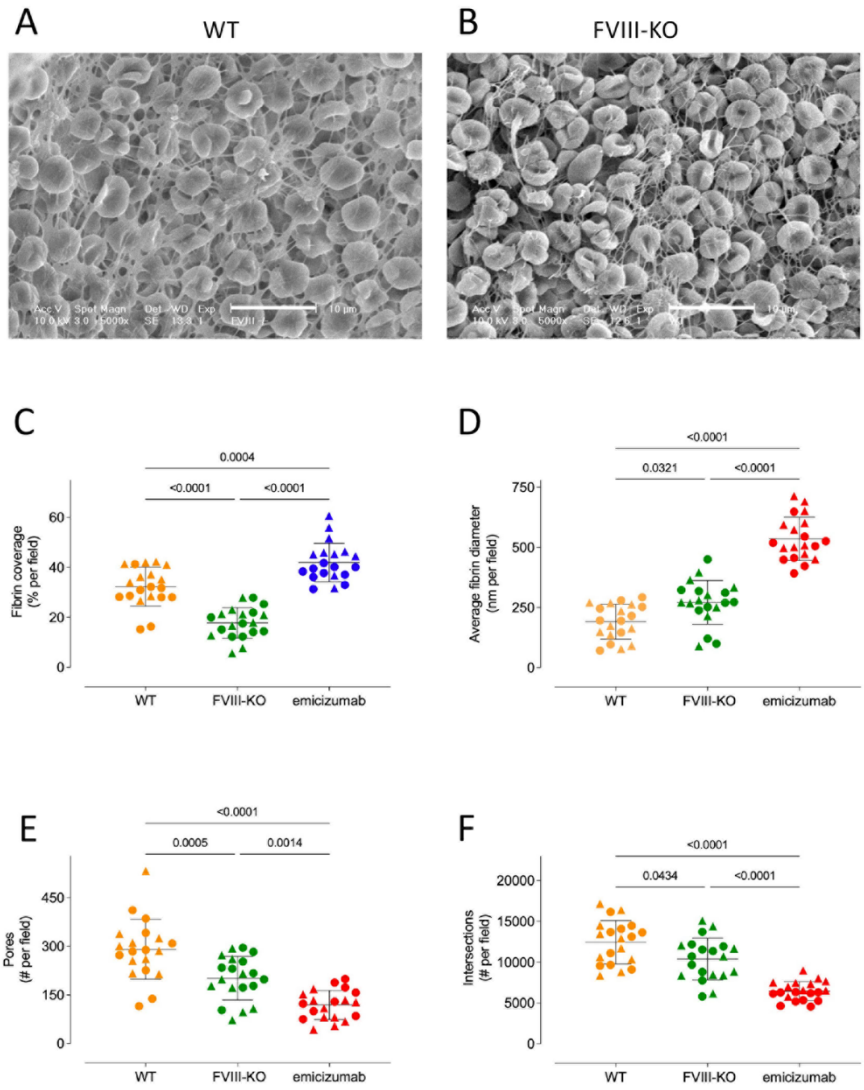

Legend Supplementary Figure S3: Scanning-EM imaging of *in vivo* generated fibrin networks. *Panel A-B:* Tail fragments obtained 10 min after TVT were prepared for scanning-EM using standard pre-fixation with 4% glutaraldehyde and 1% OsO4 and dehydration. Presented are representative images of wild-type (WT; *panel A*) and FVIII-deficient (FVIII-KO; *panel B*) mice. Scale bars represent 10 microns. *Panels C-F:* ImageJ-plugin software was used to determine fibrin coverage (% *per* field; *panel C*), average fibrin diameter (in micron *per* field; *panel D*), number of pores *per* field (*panel E*) and the number of intersections *per* field (panel *F*). For each graph, 2 mice were included (round and triangle symbols) and 10 fields *per* mouse were examined. Each symbol represents the result of a single field. Data for emicizumab (presented in Figure 4D-G) are included for comparison. Statistical analysis was performed using One-way ANOVA with Tukey's test for multiple comparisons.

Supplementary figure S4

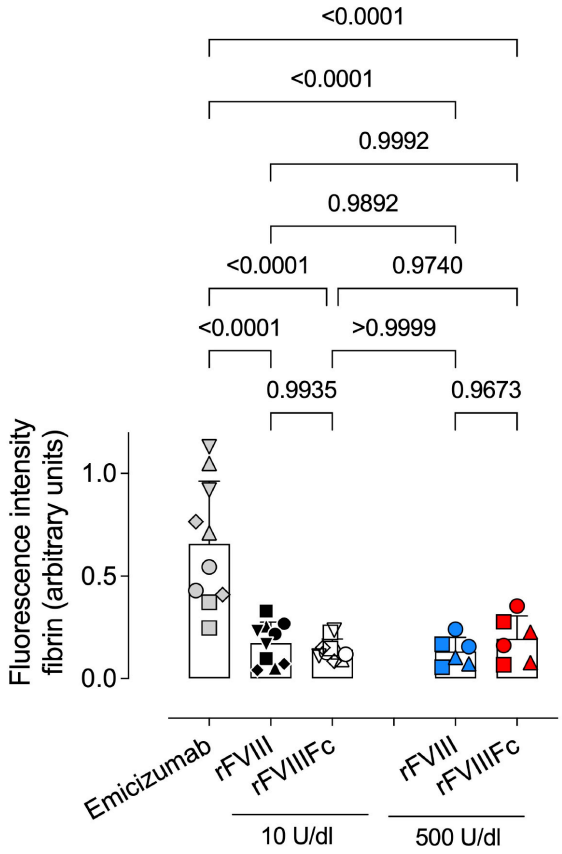

Legend Supplementary figure S4: Fibrin content within the injured area. Tail tissue sections obtained 10 min after TVT of FVIII-deficient mice that were given rFVIII, rFVIIIFc or emicizumab were prepared for immunofluorescence staining using an anti-mouse fibrin antibody. Plasma concentrations at the start of the procedure were 10 IU/dl or 500 IU/dl for rFVIII (black and blue symbols, respectively) and rFVIIIFc (white and red symbols, respectively) and 55 μg/ml for emicizumab (grey symbols). For each condition, two non-subsequent tissue sections of five mice (represented by square, round, diamond, up-triangle and down-triangle symbols) were analyzed using ImageJ-software for the fluorescence intensity. Statistical analysis was performed using one-way ANOVA with Tukey's corrections for multiple comparisons. Each symbol represents a tissue section of an individual mice, and mean±SD are indicated for each condition. Data for emicizumab and 10 IU/dl for rFVIII and rFVIIIFc are identical to those presented in figure 5.

Supplementary references

1. Bi L, Lawler AM, Antonarakis SE, High KA, Gearhart JD, Kazazian HH, Jr. Targeted disruption of the mouse factor VIII gene produces a model of haemophilia A. Nat Genet. 1995;10(1):119-21.
2. Ferriere S, Peyron I, Christophe OD, et al. A hemophilia A mouse model for the in vivo assessment of emicizumab function. Blood. 2020;136(6):740-748.
3. Johansen PB, Tranholm M, Haaning J, Knudsen T. Development of a tail vein transection bleeding model in fully anaesthetized haemophilia A mice - characterization of two novel FVIII molecules. Haemophilia. 2016.
4. Takaku Y, Suzuki H, Kawasaki H, et al. A modified 'NanoSuit(R)' preserves wet samples in high vacuum: direct observations on cells and tissues in field-emission scanning electron microscopy. R Soc Open Sci. 2017;4(3):160887.
5. Wohner N, Muczynski V, Mohamadi A, et al. Macrophage scavenger receptor SR-AI contributes to the clearance of von Willebrand factor. Haematologica. 2018;103(4):728-737.
6. Crozet F, Letort G, Bulteau R, et al. Filopodia-like protrusions of adjacent somatic cells shape the developmental potential of oocytes. Life Sci Alliance. 2023;6(6) e202301963.